Title
Pathogenic conversion of Foxp3+ T cells into TH17 cells in autoimmune arthritis

Journal
Nature Medicine, 20(1)

ISSN
1078-8956

Authors
Komatsu, Noriko
Okamoto, Kazuo
Sawa, Shinichiro
et al.

Publication Date
2014

DOI
10.1038/nm.3432

Peer reviewed

nature medicine

Pathogenic conversion of Foxp3$^+$ T cells into T_H17 cells in autoimmune arthritis

Noriko Komatsu[1,2], Kazuo Okamoto[1,2], Shinichiro Sawa[1,2], Tomoki Nakashima[2–4], Masatsugu Oh-hora[3–5], Tatsuhiko Kodama[6], Sakae Tanaka[7], Jeffrey A Bluestone[8] & Hiroshi Takayanagi[1,2,9]

Autoimmune diseases often result from an imbalance between regulatory T (T_{reg}) cells and interleukin-17 (IL-17)-producing T helper (T_H17) cells; the origin of the latter cells remains largely unknown. Foxp3 is indispensable for the suppressive function of T_{reg} cells, but the stability of Foxp3 has been under debate. Here we show that T_H17 cells originating from Foxp3$^+$ T cells have a key role in the pathogenesis of autoimmune arthritis. Under arthritic conditions, CD25^{lo}Foxp3$^+$CD4$^+$ T cells lose Foxp3 expression (herein called exFoxp3 cells) and undergo transdifferentiation into T_H17 cells. Fate mapping analysis showed that IL-17–expressing exFoxp3 T (exFoxp3 T_H17) cells accumulated in inflamed joints. The conversion of Foxp3$^+$CD4$^+$ T cells to T_H17 cells was mediated by synovial fibroblast-derived IL-6. These exFoxp3 T_H17 cells were more potent osteoclastogenic T cells than were naive CD4$^+$ T cell–derived T_H17 cells. Notably, exFoxp3 T_H17 cells were characterized by the expression of Sox4, chemokine (C-C motif) receptor 6 (CCR6), chemokine (C-C motif) ligand 20 (CCL20), IL-23 receptor (IL-23R) and receptor activator of NF-κB ligand (RANKL, also called TNFSF11). Adoptive transfer of autoreactive, antigen-experienced CD25^{lo}Foxp3$^+$CD4$^+$ T cells into mice followed by secondary immunization with collagen accelerated the onset and increased the severity of arthritis and was associated with the loss of Foxp3 expression in the majority of transferred T cells. We observed IL-17$^+$Foxp3$^+$ T cells in the synovium of subjects with active rheumatoid arthritis (RA), which suggests that plastic Foxp3$^+$ T cells contribute to the pathogenesis of RA. These findings establish the pathological importance of Foxp3 instability in the generation of pathogenic T_H17 cells in autoimmunity.

Foxp3-expressing T_{reg} cells have an essential role in suppressing immune responses[1–5]. Mice deficient in Foxp3 develop fatal autoimmune disease[3,4], and continuous expression of Foxp3 throughout life prevents autoimmunity[6]. Thus, the stability of Foxp3 expression influences the balance between tolerance and autoimmunity, as well as the efficacy of T_{reg} cell–based therapies. The instability of Foxp3 may underlie the pathogenesis of autoimmune diabetes and lethal protozoa infection[7–9], but this concept has been challenged by a report showing that Foxp3 expression is stable in *in vivo* disease models, including autoimmune arthritis[10]. A debate has arisen as to whether the plasticity of Foxp3-expressing T_{reg} cells is pathologically relevant. T_{reg} cell development and function are regulated by IL-2, which binds to the receptor complex containing IL-2Rα (also called CD25). It was recently shown that Foxp3$^+$ cells are comprised of Foxp3-stable CD25^{hi} and Foxp3-unstable CD25^{lo} populations[11,12], the former of which is composed of *bona fide* T_{reg} cells with sustained Foxp3 expression[11]. However, the pathological importance of the latter Foxp3-unstable CD25^{lo} population remains unclear.

RESULTS

T_H17 cells arise from CD25^{lo}Foxp3$^+$ T cells in arthritis

To evaluate the *in vivo* stability of Foxp3 in Foxp3$^+$CD4$^+$ T cells and its impact on collagen-induced arthritis (CIA), we adoptively transferred CD25^{hi}Foxp3$^+$CD4$^+$ or CD25^{lo}Foxp3$^+$CD4$^+$ T cells into mice that we immunized with type II collagen 3 weeks before. One day after transfer, we subjected the mice to secondary immunization with collagen. We efficiently obtained Foxp3$^+$ cells by sorting hCD2$^+$ cells from *Foxp3*^{hCD2} knock-in mice[11]. hCD2-mediated enrichment of Foxp3$^+$ cells enabled us to isolate CD25^{lo}Foxp3$^+$ cells with high purity (**Supplementary Fig. 1**). We found that the transfer of CD25^{hi}Foxp3$^+$CD4$^+$, but not CD25^{lo}Foxp3$^+$CD4$^+$, T cells reduced joint swelling (**Fig. 1a**) and bone destruction (**Fig. 1b**) without affecting the production of collagen-specific antibodies (**Supplementary Fig. 2**). To examine the stability of Foxp3, we labeled donor CD25^{hi}Foxp3$^+$CD4$^+$ or CD25^{lo}Foxp3$^+$CD4$^+$ T cells with carboxyfluorescein succinimidyl ester (CFSE) and monitored Foxp3 expression in donor-derived (CFSE$^+$) CD4$^+$ T cells 1 week after secondary immunization. The majority of CD25^{hi}Foxp3$^+$CD4$^+$ T cells

[1]Department of Immunology, Graduate School of Medicine and Faculty of Medicine, The University of Tokyo, Bunkyo-ku, Tokyo, Japan. [2]Japan Science and Technology Agency (JST), Exploratory Research for Advanced Technology (ERATO) Program, Takayanagi Osteonetwork Project, Bunkyo-ku, Tokyo, Japan. [3]Department of Cell Signaling, Graduate School of Medical and Dental Sciences, Tokyo Medical and Dental University, Bunkyo-ku, Tokyo, Japan. [4]JST, Precursory Research for Embryonic Science and Technology Program, Bunkyo-ku, Tokyo, Japan. [5]Global Center of Excellence (GCOE) Program, International Research Center for Molecular Science in Tooth and Bone Diseases, Bunkyo-ku, Tokyo, Japan. [6]Laboratory for Systems Biology and Medicine, Research Center for Advanced Science and Technology, The University of Tokyo, Meguro-ku, Tokyo, Japan. [7]Department of Orthopaedic Surgery, Faculty of Medicine, The University of Tokyo, Tokyo, Japan. [8]Diabetes Center, University of California, San Francisco, San Francisco, California, USA. [9]Centre for Orthopaedic Research, School of Surgery, The University of Western Australia, Nedlands, Western Australia, Australia. Correspondence should be addressed to H.T. (takayana@m.u-tokyo.ac.jp).

Received 31 August; accepted 19 November; published online 22 December 2013; doi:10.1038/nm.3432

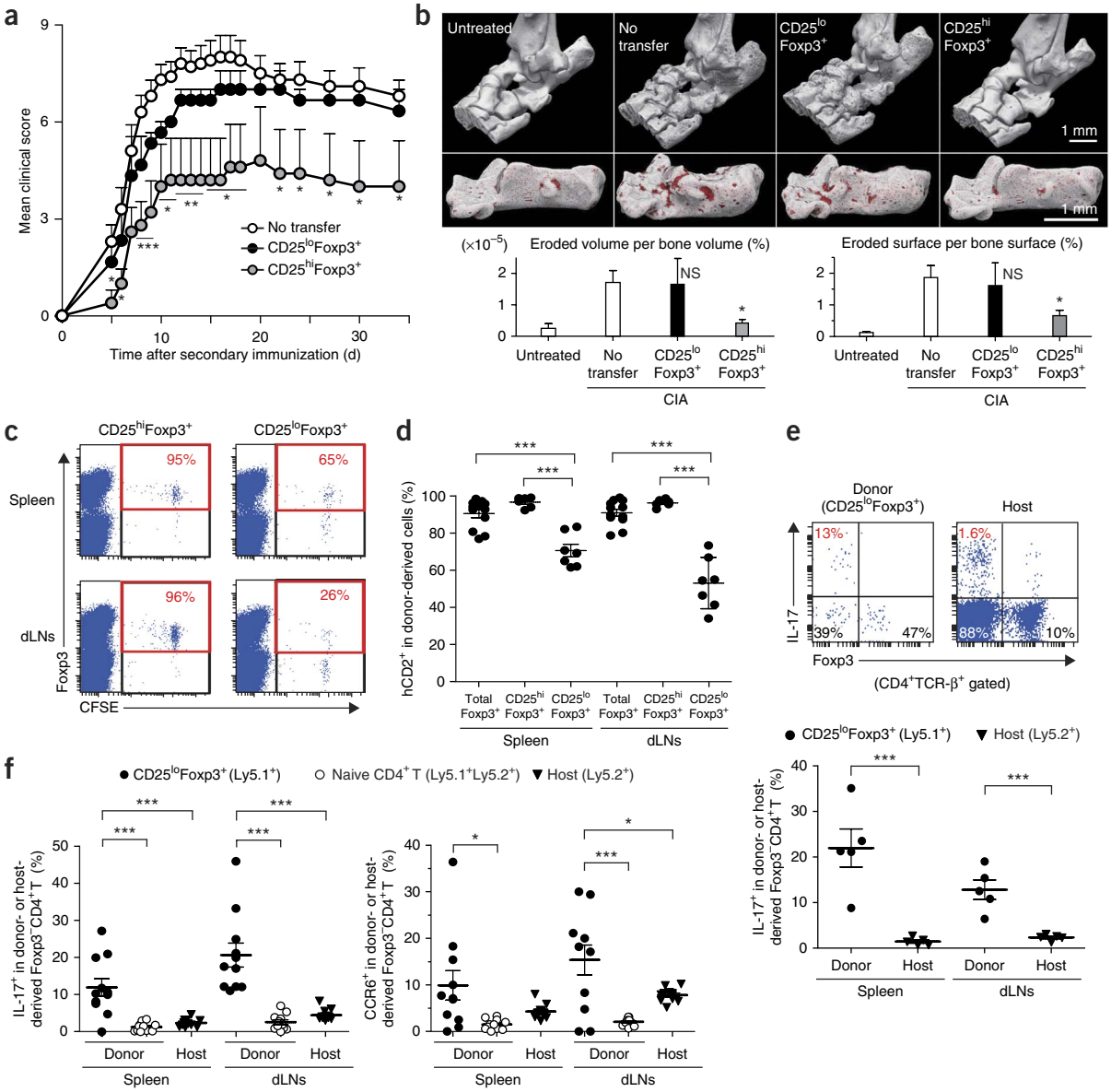

Figure 1 CD25^{lo}Foxp3^{+} T cells are unstable Foxp3^{+} T cells that convert to T_H17 cells under arthritic conditions. (**a**,**b**) Clinical score (**a**) and microcomputed tomography analysis of calcaneus in the ankle joints (**b**) of immunized DBA/1 mice adoptively transferred with 5×10^5 CD25^{hi} (**a**, $n = 3$; **b**, $n = 6$) or CD25^{lo} (**a**, $n = 5$; **b**, $n = 10$) Foxp3^{+}CD4^{+} T cells purified from untreated DBA/1 *Foxp3*^{hCD2} mice. (**c**) Frequency of Foxp3^{+} cells in CFSE^{+} donor-derived T cells. Representative data of five mice are shown. (**d**,**e**) Results from the immunized C57BL/6 Ly5.2 mice that were adoptively transferred with total hCD2^{+} ($n = 12$), CD25^{hi} ($n = 6$) or CD25^{lo} ($n = 7$) Foxp3^{+}CD4^{+} T cells from untreated B6.Ly5.1 *Foxp3*^{hCD2} mice. (**d**) Frequency of hCD2^{+} cells in donor-derived CD4^{+} T cells. (**e**) Top, representative plots of Foxp3 and IL-17 expression in CD25^{lo}Foxp3^{+} donor- or host-derived CD4^{+} T cells. Bottom, quantitative analysis of the frequency of IL-17^{+} cells in Foxp3^{-}CD4^{+} T cells derived from CD25^{lo}Foxp3^{+} donor or host cells ($n = 5$). (**f**) Frequency of IL-17^{+} (left) or CCR6^{+} (right) cells in Foxp3^{-}CD4^{+} T cells derived from CD25^{lo}Foxp3^{+} (Ly5.1^{+}Ly5.2^{-}) or naive CD4^{+} T (Ly5.1^{+}Ly5.2^{+}) donor cells or host cells (Ly5.1^{-}Ly5.2^{+}) ($n = 10$). All data are shown as the mean ± s.e.m. Statistical analyses were performed using unpaired two-tailed Student's *t* test (*$P < 0.05$, **$P < 0.01$, ***$P < 0.005$; NS, not significant). Each dot indicates a single mouse.

(>95%) retained Foxp3 expression, but CD25^{lo}Foxp3^{+}CD4^{+} T cells lost Foxp3 expression in the spleen (35%) and draining lymph nodes (dLNs) (75%) under arthritic conditions (**Fig. 1c**). These results suggest that the transferred CD25^{lo}Foxp3^{+}CD4^{+} T cells failed to inhibit inflammation and bone destruction because of their loss of Foxp3.

To follow the transferred cells for a longer period of time, we used donor T cells from B6 Ly5.1^{+} *Foxp3*^{hCD2} congenic mice and analyzed Foxp3 and IL-17 expression 2 weeks after secondary immunization in donor-derived Ly5.1^{+}CD4^{+} T cells in host mice with arthritis. The majority of transferred total Foxp3^{+} or CD25^{hi}Foxp3^{+} T cells retained Foxp3 expression, which is consistent with a previous report[10]. In contrast, when we purified and transferred CD25^{lo}Foxp3^{+}CD4^{+} T cells to the arthritic mice, these cells lost Foxp3 expression (30–50%) (**Fig. 1d**), and the percentage of IL-17–expressing cells in the donor-derived Foxp3^{-}CD4^{+} T cells (10–25%) was much greater than that in host-derived Foxp3^{-}CD4^{+} T cells (<3%) (**Fig. 1e** and **Supplementary Fig. 3**). Thus CD25^{lo}Foxp3^{+}CD4^{+} T cells preferentially lose Foxp3 and produce IL-17 in arthritic mice after adoptive transfer.

To determine the contribution of naive CD4^{+} and CD25^{lo}Foxp3^{+}CD4^{+} T cells to T_H17 cell development under arthritic

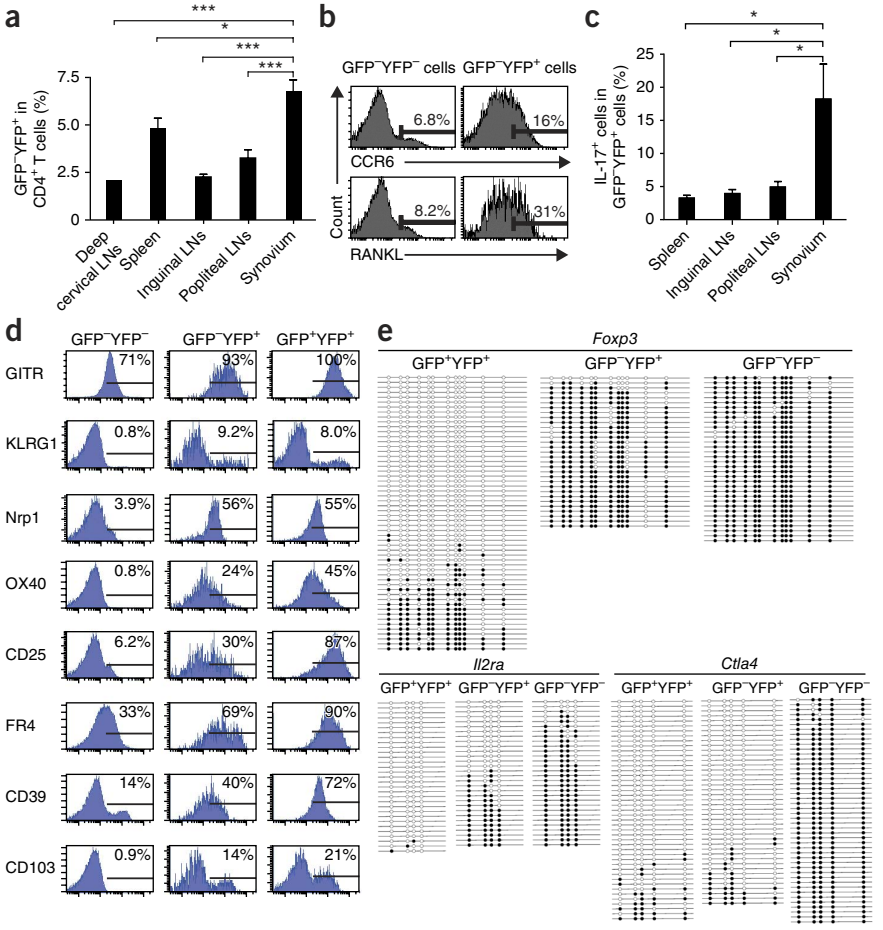

Figure 2 Localization, marker gene expression and DNA methylation status of exFoxp3 T cells in arthritic mice. Results are shown from fate mapping analyses of arthritic Foxp3-GFP-Cre × ROSA26-YFP mice that were performed 2 weeks after secondary immunization. (**a**) Frequency of exFoxp3 (GFP⁻YFP⁺) cells in CD4⁺ T cells isolated from the indicated location ($n = 3$ for deep cervical LNs, $n = 8$ for all other groups). (**b**) Expression of CCR6 and RANKL in the indicated T cell populations in popliteal lymph nodes. Representative data of six independent experiments are shown. (**c**) Frequency of IL-17⁺ cells in the GFP⁻YFP⁺ cell population ($n = 6$). (**d**) Expression of multiple T_{reg} cell phenotypic markers in exFoxp3 T cells. Representative data of six independent experiments are shown. The percentages in each plot show the frequency of positive cells (indicated by the horizontal lines). (**e**) CpG methylation of the *Foxp3*, *Il2ra* and *Ctla4* loci in exFoxp3 (GFP⁻YFP⁺), GFP⁺YFP⁺ and GFP⁻YFP⁻CD4⁺ T cells. A horizontal row within each box corresponds to one sequenced clone in which specific CpGs were methylated (closed) or demethylated (open). All data are shown as the mean ± s.e.m. Statistical analyses were performed using unpaired two-tailed Student's *t* test (*$P < 0.05$, ***$P < 0.005$).

conditions, we transferred Ly5.1⁺Ly5.2⁺ naive CD4⁺ and Ly5.1⁺CD25^{lo}Foxp3⁺CD4⁺ T cells into immunized Ly5.2⁺ mice, which we analyzed 2 weeks after secondary immunization. CD25^{lo}Foxp3⁺ donor-derived Ly5.1⁺Foxp3⁻CD4⁺ T cells expressed the T_H17 markers IL-17 and CCR6 (refs. 13,14) to a much greater extent than did naive CD4⁺ donor-derived or host-derived Foxp3⁻CD4⁺ T cells (**Fig. 1f**). These findings suggest that under arthritic conditions, CD25^{lo}Foxp3⁺CD4⁺ T cells are prone to differentiate into T_H17 cells that are known to have a key pathological role in arthritis[13–18].

Characterization of exFoxp3 T cells in arthritic mice

To monitor the localization of exFoxp3 T cells *in vivo*, we crossed *Foxp3* bacterial artificial chromosome transgenic mice expressing the GFP-Cre recombinase fusion protein[7] with ROSA26-YFP reporter mice[19]. GFP indicates cells that are currently expressing Foxp3, whereas YFP marks cells that are expressing or did express Foxp3. Under arthritic conditions, the percentage of exFoxp3 (GFP⁻YFP⁺) cells (as a proportion of total CD4⁺ T cells) was higher in joints than in other lymphoid organs (**Fig. 2a** and **Supplementary Fig. 4**), suggesting a preferential accumulation of exFoxp3 T cells in the synovium. In addition, exFoxp3 (GFP⁻YFP⁺) T cells expressed higher levels of CCR6 and RANKL than did GFP⁻YFP⁻ T cells in popliteal LNs (**Fig. 2b**). Notably, the percentage of IL-17⁺ cells among exFoxp3 T cells was highest in arthritic joints (**Fig. 2c**). These results collectively indicate that *in vivo*, exFoxp3 T cells acquire an activated T_H17 phenotype (exFoxp3 T_H17 cells) and accumulate in the inflamed synovium.

Instability of Foxp3⁺ T_{reg} cells under pathological conditions *in vivo* has been contentious, as the origin of this Foxp3-unstable population remains unclear. There are three possibilities for the origin of exFoxp3 T cells: thymus-derived T_{reg} (tT_{reg}) cells, peripherally derived T_{reg} (pT_{reg}) cells and activated conventional T cells that transiently express Foxp3 (refs. 20,21). T_{reg} cells are defined by their suppressive function and are characterized by the expression and demethylated status of Foxp3 and other T_{reg} cell signature genes[20,22]. Flow cytometric analysis indicated that GITR (also called TNFRSF18), neuropilin 1 (Nrp1) and killer cell lectin-like receptor subfamily G member 1 (KLRG1) were similarly expressed by exFoxp3 T cells and GFP⁺YFP⁺ T cells (**Fig. 2d**). exFoxp3 T cells also expressed CD25, folate receptor 4 (FR4), OX40 (also called TNFRSF4), CD39 (also called ENTPD1), CD103 (also called ITGAE) and cytotoxic T lymphocyte–associated protein 4 (CTLA-4), albeit to a lesser extent compared to GFP⁺YFP⁺ T cells (**Fig. 2d** and **Supplementary Fig. 5**). Thus, although the expression level of a few T_{reg} marker genes, including CD25 and FR4, was lower in exFoxp3 T cells than in GFP⁺YFP⁺ T cells, exFoxp3 T cells expressed most of the phenotypic T_{reg} markers and were distinguishable from activated conventional T cells that transiently express Foxp3 (**Fig. 2d**).

Methylation analysis of the *Foxp3*, *Il2ra* and *Ctla4* loci[22] in exFoxp3 T cells isolated from spleens and dLNs of arthritic mice revealed that the *Foxp3* locus was largely methylated and the *Il2ra* locus was partially methylated in exFoxp3 (GFP⁻YFP⁺) T cells (**Fig. 2e**). As the *Foxp3* locus in tT_{reg} cells is known to be demethylated[22], the data suggest that exFoxp3 T cells are not derived from tT_{reg} cells. The *Ctla4* locus of exFoxp3 T cells was demethylated, making these cells distinct from effector memory T cells and *in vitro*–induced T_{reg} cells[22].

Genome-wide expression analysis showed that exFoxp3 T_H17 cells highly express *Cxcr5*, *Ccr8*, *Rora* and *Rorc*, which are preferentially expressed in pT_{reg} cells that are generated through antigen delivery or in T_{reg} cells in the gut lamina propria[23] (**Supplementary Fig. 6**), but have lower expression of *Ikzf2* (encoding Helios) (**Supplementary Figs. 5** and **6**). These results suggest that exFoxp3 T_H17 cells may

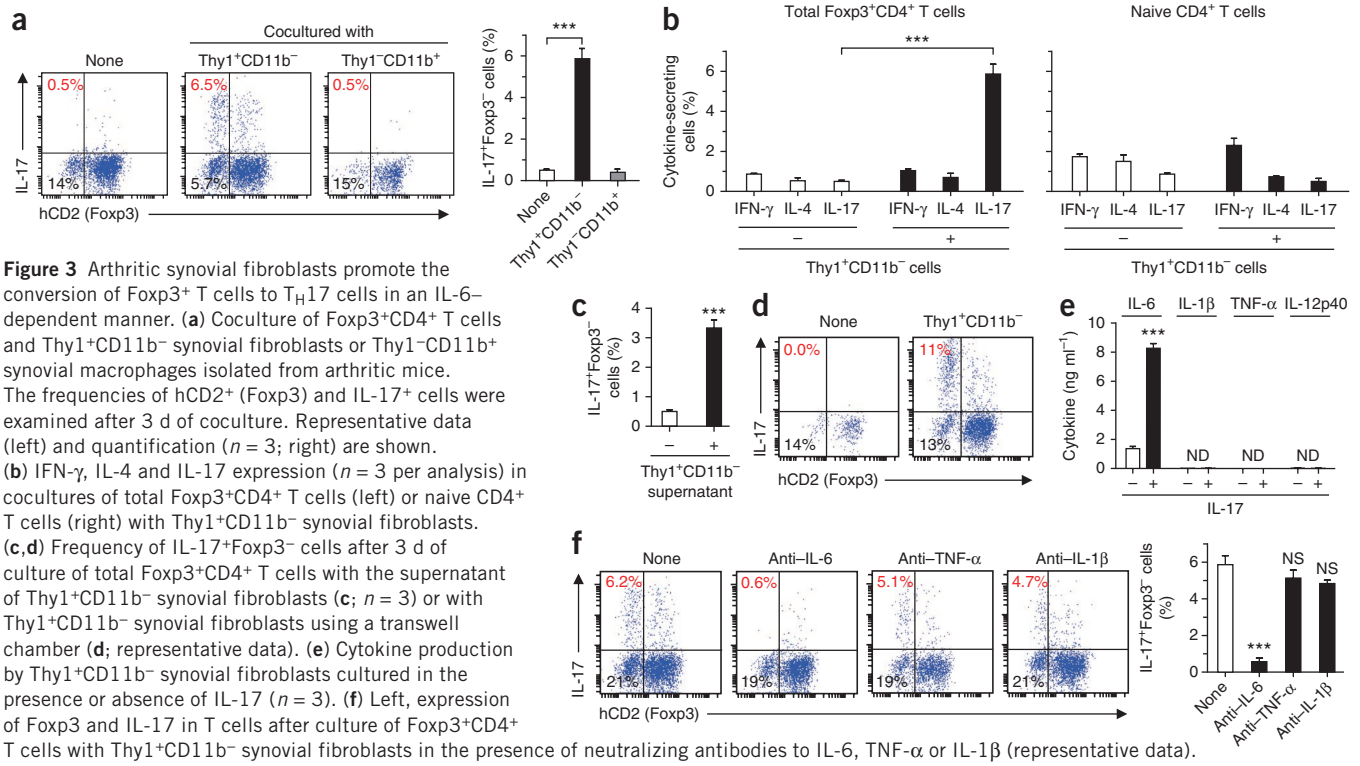

Figure 3 Arthritic synovial fibroblasts promote the conversion of Foxp3+ T cells to T_H17 cells in an IL-6–dependent manner. (**a**) Coculture of Foxp3+CD4+ T cells and Thy1+CD11b− synovial fibroblasts or Thy1−CD11b+ synovial macrophages isolated from arthritic mice. The frequencies of hCD2+ (Foxp3) and IL-17+ cells were examined after 3 d of coculture. Representative data (left) and quantification ($n = 3$; right) are shown. (**b**) IFN-γ, IL-4 and IL-17 expression ($n = 3$ per analysis) in cocultures of total Foxp3+CD4+ T cells (left) or naive CD4+ T cells (right) with Thy1+CD11b− synovial fibroblasts. (**c**,**d**) Frequency of IL-17+Foxp3− cells after 3 d of culture of total Foxp3+CD4+ T cells with the supernatant of Thy1+CD11b− synovial fibroblasts (**c**; $n = 3$) or with Thy1+CD11b− synovial fibroblasts using a transwell chamber (**d**; representative data). (**e**) Cytokine production by Thy1+CD11b− synovial fibroblasts cultured in the presence or absence of IL-17 ($n = 3$). (**f**) Left, expression of Foxp3 and IL-17 in T cells after culture of Foxp3+CD4+ T cells with Thy1+CD11b− synovial fibroblasts in the presence of neutralizing antibodies to IL-6, TNF-α or IL-1β (representative data). Right, quantitative analysis of the frequency of IL-17+Foxp3− cells in T cells ($n = 3$). All data are shown as the mean ± s.e.m. Statistical analyses were performed using unpaired two-tailed Student's *t* test (***$P < 0.005$; NS, not significant; ND, not detected). Data are representative of three independent experiments with triplicate culture wells.

belong to a subpopulation of pT_{reg} cells rather than tT_{reg} cells. Taken together, it is possible that exFoxp3 T cells may comprise a previously unrecognized T cell population or pT_{reg} cell–derived T cell subset that is distinct from tT_{reg} cells and activated conventional T cells. Future study of the methylation status of the *Foxp3* TSDR region in pT_{reg} cells under physiological and pathological conditions will be helpful to understand the origin of exFoxp3 T cells in more detail.

Synovial fibroblasts convert Foxp3+ T cells into T_H17 cells

Accumulation of exFoxp3 T_H17 cells in arthritic joints led us to hypothesize that cells that are resident in the joint interact with Foxp3+ cells, facilitating the conversion of Foxp3+ T cells to T_H17 cells. To explore the role of synovial cells in the regulation of *Foxp3* stability, we isolated Thy1+CD11b− cells (synovial fibroblasts) and Thy1−CD11b+ cells (synovial macrophages) from the joints of arthritic mice and cocultured them with total Foxp3+CD4+ T cells purified from unmanipulated *Foxp3*^{hCD2} mice. Coculture of Thy1+CD11b− cells, but not Thy1−CD11b+ cells, with Foxp3+CD4+ cells downregulated Foxp3 expression in Foxp3+CD4+ T cells (**Fig. 3a**). These exFoxp3 T cells upregulate IL-17 but do not express interferon-γ (IFN-γ) or IL-4 when cocultured with arthritic synovial fibroblasts (**Fig. 3a**,**b**), suggesting that arthritic synovial fibroblasts promote the conversion of Foxp3+ T cells to T_H17 cells in the joints. In contrast, when we cocultured naive CD4+ T cells with Thy1+CD11b− synovial fibroblasts, they did not differentiate into T_H17 cells (**Fig. 3b**). We detected IL-17+Foxp3+ T cells, which may appear at the transition stage during the conversion of Foxp3+ T cells to T_H17 cells, in the joints and lymph nodes of arthritic mice (**Supplementary Fig. 7**), as well as in the synovium of human subjects with RA (**Supplementary Fig. 8**).

We next investigated the mechanism by which synovial fibroblasts induce the conversion of Foxp3+CD4+ T cells into T_H17 cells. The culture supernatant of synovial fibroblasts (**Fig. 3c**) or coculture of Foxp3+CD4+ T cells with transwell-separated synovial fibroblasts (**Fig. 3d**) induced conversion into T_H17 cells, indicating that cell-cell contact is not essential for conversion. We explored the soluble factors mediating this conversion by analyzing the expression of various cytokines in the supernatant (**Fig. 3e** and data not shown) and found that IL-6 was highly produced by Thy1+CD11b− cells (**Fig. 3e**). The expression of IL-6 by arthritic synovial fibroblasts was further enhanced by IL-17, suggesting a potential positive feedback loop (**Fig. 3e**). A neutralizing antibody against IL-6, but neither an antibody to TNF-α nor one to IL-1β, inhibited the generation of T_H17 cells after the coculture of Foxp3+CD4+ T cells with synovial fibroblasts (**Fig. 3f**). These results indicate that synovial fibroblast–derived IL-6 has a crucial role in the conversion of Foxp3+CD4+ T cells to T_H17 cells.

exFoxp3 T_H17 cells are potent osteoclastogenic T cells

To evaluate the contribution of T_H17 cells of a Foxp3+ T cell origin to the bone destruction that occurs in arthritis, we examined their ability to induce osteoclastogenesis by counting the number of osteoclasts defined by TRAP+ multinucleated cells (MNCs) and the expression of RANKL, a cytokine that is essential for osteoclast differentiation[16], in comparison with both naive CD4+ T cell–derived T_H17 cells and Foxp3+ T cells. We found that exFoxp3 T_H17 cells had higher osteoclastogenic ability than naive CD4+ T cell–derived T_H17 cells in a coculture of synovial fibroblasts and bone marrow–derived monocyte and macrophage precursor cells (BMMs) (**Fig. 4a**,**b**). Foxp3+ T cells cultured in the presence of IL-2 did not have osteoclastogenic ability, which is consistent with a previous report[24]. We confirmed these findings further using *Foxp3*^{hCD2} mice crossed with IL-17–GFP knock-in mice, which enabled us to purify IL-17–expressing cells (**Supplementary Fig. 9**).

The osteoclastogenic ability of T_H17 cells has been attributed mainly to their production of IL-17, which stimulates RANKL expression in fibroblasts, as T_H17 cells alone cannot induce osteoclastogenesis despite their RANKL expression[25]. However, *Il17a*$^{-/-}$ exFoxp3 T cells that were differentiated under T_H17-polarizing conditions still induced osteoclastogenesis, suggesting a potential contribution of T cell–derived RANKL or RANKL-inducing cytokines other than IL-17A (**Fig. 4b**). We observed that exFoxp3 T_H17 cells expressed higher amounts of RANKL than did naive CD4$^+$ T cell–derived T_H17 cells (**Fig. 4c**) and coculture with synovial fibroblasts further enhanced

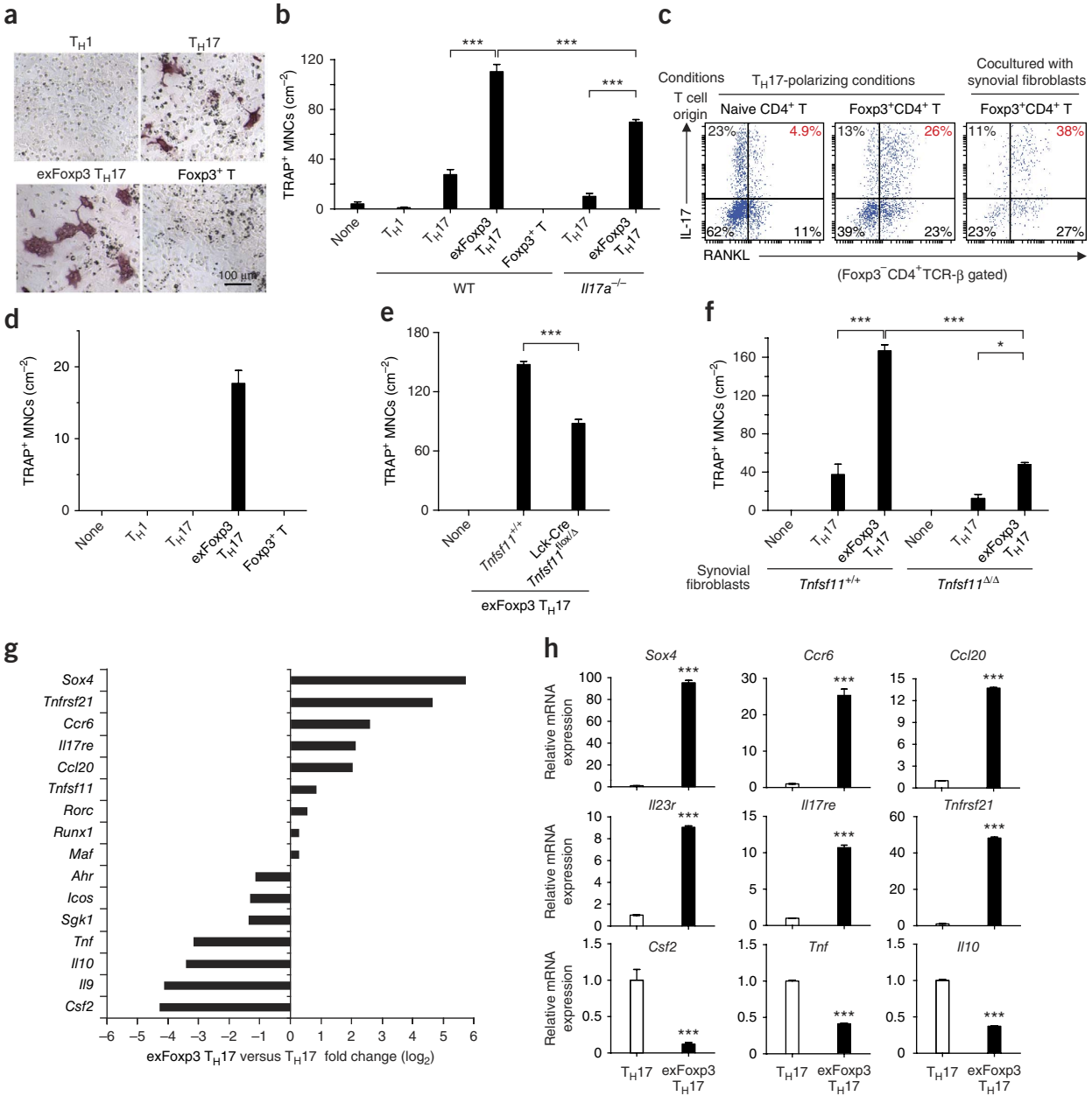

Figure 4 exFoxp3 T_H17 cells are osteoclastogenic T cells with distinct gene profiles. (**a**,**b**) Osteoclast differentiation in a coculture of BMMs, Thy1$^+$CD11b$^-$ CIA synovial fibroblasts and the T cell subsets indicated. exFoxp3 T_H17 indicates Foxp3$^-$ T cells developed from Foxp3$^+$ T cells under T_H17-polarizing conditions in this experiment. (**a**) Representative tartrate-resistant acid phosphatase (TRAP) staining. (**b**) Number of osteoclasts (TRAP$^+$ MNCs) ($n = 3$ for exFoxp3 T_H17 and Foxp3$^+$ T cells, $n = 4$ for *Il17a*$^{-/-}$ T_H17 cells, $n = 6$ for all other groups). WT, wild type. (**c**) Representative FACS profiles of RANKL and IL-17 expression in naive CD4$^+$ T cell–derived T_H17 cells (left) and exFoxp3 T_H17 cells (middle and right) that differentiated under the conditions indicated. (**d**) Number of osteoclasts (TRAP$^+$ MNCs) in a coculture of BMMs and the T cell subsets indicated ($n = 3$). (**e**,**f**) Number of osteoclasts (TRAP$^+$ MNCs) in a coculture of BMMs, synovial fibroblasts and the T cell subsets indicated. (**e**) Analysis using exFoxp3 T_H17 cells derived from *Tnfsf11*$^{+/+}$ *Foxp3*^{hCD2} or Lck-Cre *Tnfsf11*$^{flox/\Delta}$ *Foxp3*^{hCD2} mice. (**f**) Analysis using *Tnfsf11*$^{+/+}$ or *Tnfsf11*$^{\Delta/\Delta}$ arthritic synovial fibroblasts. (**g**) Microarray analysis of selected T_H17-related genes in exFoxp3 T_H17 cells and T_H17 cells. IL-17^{GFP+} *Foxp3*$^{hCD2-}$ cells developed from naive CD4$^+$ T cells or Foxp3$^+$CD4$^+$ T cells under T_H17-polarizing conditions were used as the T_H17 cells and exFoxp3 T_H17 cells, respectively. The mean fold change of three independent experiments is shown. (**h**) Quantitative RT-PCR analysis of differentially expressed genes in T_H17 cells and exFoxp3 T_H17 cells ($n = 3$). All data are representative of three independent experiments with triplicate culture wells and are shown as the mean ± s.e.m. Statistical analyses were performed using unpaired two-tailed Student's *t* test (*$P < 0.05$, ***$P < 0.005$).

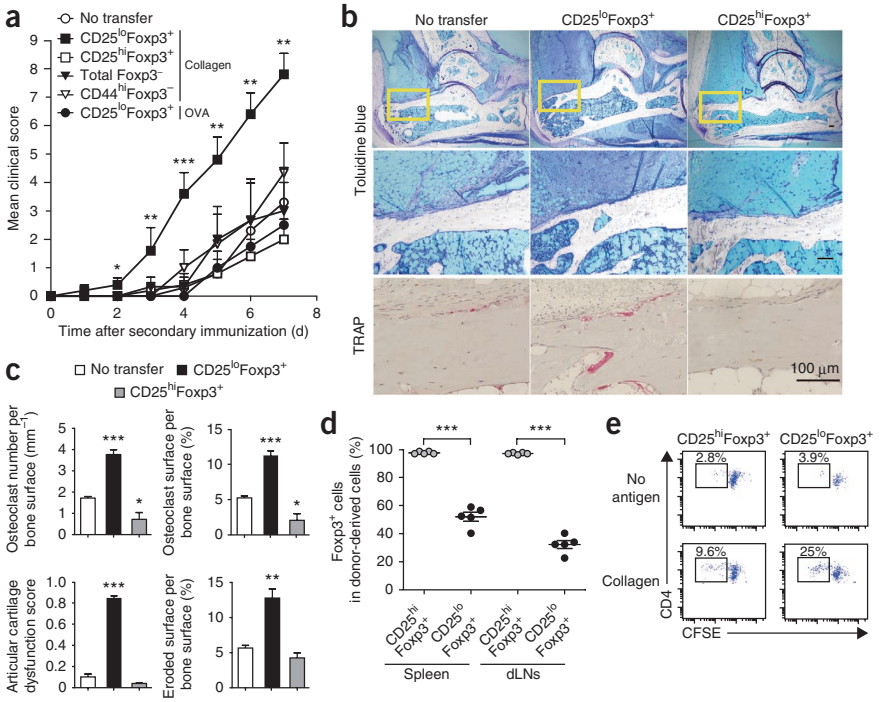

Figure 5 Pathogenic role of exFoxp3 T cells to arthritis *in vivo*. (**a**–**c**) Clinical score (**a**), histological analysis (**b**) and bone morphometric analysis (**c**) of the ankle joints of DBA/1 *Foxp3*^{hCD2} mice adoptively transferred with the indicated T cell subsets that were purified from spleens and dLNs of collagen-immunized mice ($n = 3$ for total Foxp3$^-$ cells, $n = 5$ for CD25^{lo}Foxp3$^+$ and CD25^{hi}Foxp3$^+$ cells, $n = 6$ for CD44^{hi}Foxp3$^-$ cells) or OVA-immunized mice ($n = 4$). In **b**, toluidine blue (top and middle) and TRAP (bottom) staining of ankle joints were performed. The middle row is a magnification of the boxed areas in the top row. Scale bars, 100 μm. In **c**, the quantitative bone morphometric analysis was performed using histological sections ($n = 3$). Osteoclast number per bone surface (top left), osteoclast surface per bone surface (top right), articular cartilage dysfunction score (bottom left) and eroded surface per bone surface (bottom right) are shown. (**d**) Frequency of Foxp3$^+$ cells in donor-derived CFSE$^+$CD4$^+$ T cells 1 week after secondary immunization ($n = 5$). (**e**) *In vitro* proliferative responses to type II collagen of CD25^{hi}Foxp3$^+$ or CD25^{lo}Foxp3$^+$ T cells purified from the spleens and dLNs of collagen-immunized mice. The numbers indicate the frequency of proliferating cells as determined by CFSE dilution. Representative data of more than three independent experiments are shown. All data are shown as the mean ± s.e.m. Statistical analyses were performed using one-way analysis of variance with Newman-Keuls multiple comparison test (**a**) or unpaired two-tailed Student's *t* test (**c**,**d**) (*$P < 0.05$, **$P < 0.01$, ***$P < 0.005$).

the expression of RANKL in exFoxp3 T$_H$17 cells (**Fig. 4c**). Notably, exFoxp3 T$_H$17 cells alone induced osteoclastogenesis from BMMs, even in the absence of synovial fibroblasts (**Fig. 4d**). To elucidate the relative contribution of RANKL in exFoxp3 T$_H$17 cells and synovial fibroblasts, we used exFoxp3 T$_H$17 cells from Lck-Cre *Tnfsf11* (encoding RANKL)$^{flox/\Delta}$ *Foxp3*^{hCD2} mice or *Tnfsf11*-deficient synovial fibroblasts in the T cell and synovial fibroblast coculture system. Although RANKL expressed on synovial fibroblasts has a major role in promoting osteoclastogenesis, RANKL expressed by exFoxp3 T$_H$17 cells was able to induce osteoclastogenesis, even in the absence of RANKL expression on synovial fibroblasts (**Fig. 4e**,**f**).

To gain molecular insight into the pathogenicity of exFoxp3 T$_H$17 cells, we performed GeneChip analysis of exFoxp3 T$_H$17 cells and naive CD4$^+$-derived T$_H$17 cells. exFoxp3 T$_H$17 cells expressed higher amounts of *Ccr6*, *Ccl20*, *Il23r*, *Il17re*, *Tnfrsf21*, *Vcam1*, *Rorc* and *Tnfsf11* but lower amounts of *Csf2*, *Tnf*, *Il10* and *Sgk1* than T$_H$17 cells (**Fig. 4g**,**h** and **Supplementary Fig. 10**). These data suggest that exFoxp3 T$_H$17 cells are not identical to any known pathogenic T$_H$17 cell subsets[26–29]. Notably, we found that exFoxp3 T$_H$17 cells specifically and highly express the transcription factor Sox4, which positively regulates RORγt (encoded by *Rorc*)[30] and enhances lymphoid cell survival[31]. The high expression of molecules that are involved in proliferation, such as *Pik3r3*, and the high frequency of Ki-67$^+$ cells in exFoxp3 T cells (**Supplementary Figs. 10** and **11**) suggest that under arthritic conditions, exFoxp3 T$_H$17 cells are proliferative. Thus, exFoxp3 T$_H$17 cells comprise a new pathogenic T$_H$17 cell subset that expresses Sox4, CCR6, CCL20, IL-23R, IL-17RE and RANKL.

Autoreactive CD25^{lo}Foxp3$^+$ T cells promote arthritis

Self tolerance is maintained by thymic-derived stable Foxp3$^+$CD4$^+$ T cells, which have a higher affinity for self antigens[32,33]. We hypothesized that unstable Foxp3$^+$CD4$^+$ T cells also contain self-reactive T cells and thus exert a potent arthritogenic effect after losing Foxp3 expression. To investigate the role of autoantigen-specific exFoxp3 T cells, we purified CD25^{lo}Foxp3$^+$, CD25^{hi}Foxp3$^+$, total Foxp3$^-$ and effector memory CD44^{hi}Foxp3$^-$CD4$^+$ T cells from collagen-immunized DBA/1 *Foxp3*^{hCD2} mice, which harbor collagen-specific T cells. After CFSE labeling, we transferred these cells into immunized mice 1 d before secondary immunization. Notably, CD25^{lo}Foxp3$^+$ T cells accelerated the onset and increased the severity of arthritic symptoms more than total Foxp3$^-$ or CD44^{hi}Foxp3$^-$ CD4$^+$ T cells (**Fig. 5a**–**c**). In contrast, the transfer of CD25^{hi}Foxp3$^+$CD4$^+$ T cells markedly inhibited osteoclast formation. More than half (50–70%) of the CD25^{lo}Foxp3$^+$ T cells lost Foxp3 expression, whereas almost all (>96%) of the CD25^{hi}Foxp3$^+$ cells retained Foxp3 expression (**Fig. 5d**). CD25^{lo}Foxp3$^+$ cells proliferated in response to type II collagen *in vitro* to a greater extent than did CD25^{hi}Foxp3$^+$ cells, suggesting that the CD25^{lo}Foxp3$^+$ cells contained a higher number of autoreactive T cells (**Fig. 5e**).

To further examine whether the exacerbation of arthritic symptoms elicited by CD25^{lo}Foxp3$^+$CD4$^+$ T cells is dependent on type II collagen–specific responses, we transferred CD25^{lo}Foxp3$^+$CD4$^+$ T cells from ovalbumin (OVA)-immunized mice to collagen-immunized mice. OVA-specific CD25^{lo}Foxp3$^+$CD4$^+$ T cells did not exacerbate arthritis scores (**Fig. 5a**). These results suggest that autoreactive pathogenic CD4$^+$ T cells were generated mainly from CD25^{lo}Foxp3$^+$CD4$^+$ T cells under arthritic conditions.

DISCUSSION

This study demonstrates that CD4$^+$ T$_H$17 cells with arthritogenic and autoreactive properties arise from Foxp3$^+$CD4$^+$ T cells, thus establishing the *in vivo* pathological importance of Foxp3$^+$CD4$^+$ T cell conversion to T$_H$17 cells. The pathogenic function of IL-17$^+$ exFoxp3 T cells may be enhanced by their higher affinity to self antigens, as well as their ability to accumulate and proliferate in inflamed tissues and stimulate

osteoclastogenesis. Conversion of Foxp3$^+$CD4$^+$ T cells into T_H17 cells in the periphery was promoted by arthritic synovial fibroblasts, thereby uncovering a new interaction of immune and tissue-resident mesenchymal cells in the breakdown of self tolerance. We propose that the fate of plastic Foxp3$^+$ T cells is a critical determinant of self tolerance versus autoimmunity. The balance between IL-2 and IL-6 regulates the development of T_{reg} and T_H17 cells from naive CD4$^+$ T cells[34], but the fate of plastic Foxp3$^+$ T cells may also be determined by this cytokine balance[35] (**Supplementary Fig. 12**). Blockade of IL-6 signaling increases the ratio of Foxp3$^+$ to T_H17 cells in the course of RA treatment[36], suggesting that some of the beneficial effects of these therapies may derive from regulation of the plasticity of Foxp3$^+$ T cell fate. Blockade of TNF-α also increases the ratio of T_{reg} to T_H17 cells[37,38], and it was recently reported that this effect is attributable to the recovery of T_{reg} cell function[38]. These reports suggest that regulating the balance of T_{reg} to T_H17 cells is important for the treatment of RA. Several RA-associated genes[39], including *Ptpn22*, *Ccr6* and *Tnfrsf14*, are highly expressed in exFoxp3 T_H17 cells (**Supplementary Fig. 13**), and we observed IL-17$^+$Foxp3$^+$ T cells in subjects with active RA (**Supplementary Fig. 8**), suggesting the potential role of exFoxp3 T_H17 cells in the pathogenesis of RA. Notably, we found that exFoxp3 T_H17 cells specifically express a set of surface molecules that may be useful in identifying arthritogenic T cells and may contribute to future diagnostic and therapeutic strategies for RA (**Supplementary Fig. 10d**). The presence of exFoxp3 T_H17 cells may be used as a biomarker for RA and be useful for predicting responsiveness to anti–IL-6 therapy. Further characterization of the mechanisms underlying the conversion and function of plastic Foxp3$^+$ T cells will provide new insights into the maintenance and restoration of self tolerance, and this will in turn lead to the development of new therapeutic strategies for autoimmune diseases.

METHODS

Methods and any associated references are available in the online version of the paper.

Accession codes. Microarray data have been deposited in the Gene Expression Omnibus database with accession code GSE48428.

Note: Any Supplementary Information and Source Data files are available in the online version of the paper.

ACKNOWLEDGMENTS

We are grateful to S. Hori (RIKEN Center for Integrative Medical Sciences) and Y. Iwakura (Tokyo University of Science) for providing B6.*Foxp3*^{hCD2} knock-in mice and *Il17a*$^{-/-}$ mice, respectively. We also thank T. Negishi-Koga, M. Shinohara, A. Terashima, M. Guerrini, L. Danks, M. Hayashi, T. Ando, Y. Ogiwara, N. Otsuka, T. Kato, C. Tsuda, T. Suda, A. Suematsu, S. Fukuse, Y. Wada, A. Izumi and K. Kaneki for discussion and assistance. This work was supported in part by a grant for the ERATO Takayanagi Osteonetwork Project from JST; a Grant-in-Aid for Challenging Exploratory Research from the Japan Society for the Promotion of Science (JSPS); a Grant-in-Aid for JSPS Fellows; and a grant for the GCOE Program from the Ministry of Education, Culture, Sports, Science and Technology of Japan. N.K. was supported by JSPS Research Fellowships for Young Scientists.

AUTHOR CONTRIBUTIONS

N.K. designed and performed experiments, interpreted the results and prepared the manuscript. K.O., S.S., T.N. and M.O. contributed to study design and manuscript preparation. T.K. contributed to microarray analysis. S.T. contributed to the analysis of human RA and osteoarthritis samples. J.A.B. generated Foxp3-GFP-Cre mice and contributed to study design and data interpretation. H.T. directed the project and wrote the manuscript.

COMPETING FINANCIAL INTERESTS

The authors declare no competing financial interests.

1. Sakaguchi, S. Naturally arising CD4$^+$ regulatory T cells for immunologic self-tolerance and negative control of immune responses. *Annu. Rev. Immunol.* **22**, 531–562 (2004).
2. Hori, S., Nomura, T. & Sakaguchi, S. Control of regulatory T cell development by the transcription factor Foxp3. *Science* **299**, 1057–1061 (2003).
3. Fontenot, J.D., Gavin, M.A. & Rudensky, A.Y. Foxp3 programs the development and function of CD4$^+$CD25$^+$ regulatory T cells. *Nat. Immunol.* **4**, 330–336 (2003).
4. Khattri, R., Cox, T., Yasayko, S.A. & Ramsdell, F. An essential role for Scurfin in CD4$^+$CD25$^+$ T regulatory cells. *Nat. Immunol.* **4**, 337–342 (2003).
5. Wan, Y.Y. & Flavell, R.A. Regulatory T-cell functions are subverted and converted owing to attenuated Foxp3 expression. *Nature* **445**, 766–770 (2007).
6. Kim, J.M., Rasmussen, J.P. & Rudensky, A.Y. Regulatory T cells prevent catastrophic autoimmunity throughout the lifespan of mice. *Nat. Immunol.* **8**, 191–197 (2007).
7. Zhou, X. *et al.* Instability of the transcription factor Foxp3 leads to the generation of pathogenic memory T cells *in vivo*. *Nat. Immunol.* **10**, 1000–1007 (2009).
8. Yang, X.O. *et al.* Molecular antagonism and plasticity of regulatory and inflammatory T cell programs. *Immunity* **29**, 44–56 (2008).
9. Oldenhove, G. *et al.* Decrease of Foxp3$^+$ T_{reg} cell number and acquisition of effector cell phenotype during lethal infection. *Immunity* **31**, 772–786 (2009).
10. Rubtsov, Y.P. *et al.* Stability of the regulatory T cell lineage *in vivo*. *Science* **329**, 1667–1671 (2010).
11. Miyao, T. *et al.* Plasticity of Foxp3$^+$ T cells reflects promiscuous Foxp3 expression in conventional T cells but not reprogramming of regulatory T cells. *Immunity* **36**, 262–275 (2012).
12. Komatsu, N. *et al.* Heterogeneity of natural Foxp3$^+$ T cells: a committed regulatory T-cell lineage and an uncommitted minor population retaining plasticity. *Proc. Natl. Acad. Sci. USA* **106**, 1903–1908 (2009).
13. Hirota, K. *et al.* Preferential recruitment of CCR6-expressing Th17 cells to inflamed joints via CCL20 in rheumatoid arthritis and its animal model. *J. Exp. Med.* **204**, 2803–2812 (2007).
14. Murakami, M. *et al.* Local microbleeding facilitates IL-6– and IL-17–dependent arthritis in the absence of tissue antigen recognition by activated T cells. *J. Exp. Med.* **208**, 103–114 (2011).
15. Korn, T., Bettelli, E., Oukka, M. & Kuchroo, V.K. IL-17 and Th17 cells. *Annu. Rev. Immunol.* **27**, 485–517 (2009).
16. Takayanagi, H. Osteoimmunology: shared mechanisms and crosstalk between the immune and bone systems. *Nat. Rev. Immunol.* **7**, 292–304 (2007).
17. Hashimoto, M. *et al.* Complement drives Th17 cell differentiation and triggers autoimmune arthritis. *J. Exp. Med.* **207**, 1135–1143 (2010).
18. Wu, H.J. *et al.* Gut-residing segmented filamentous bacteria drive autoimmune arthritis via T helper 17 cells. *Immunity* **32**, 815–827 (2010).
19. Srinivas, S. *et al.* Cre reporter strains produced by targeted insertion of EYFP and ECFP into the ROSA26 locus. *BMC Dev. Biol.* **1**, 4 (2001).
20. Sakaguchi, S. *et al.* The plasticity and stability of regulatory T cells. *Nat. Rev. Immunol.* **13**, 461–467 (2013).
21. Wehrens, E.J., Prakken, B.J. & van Wijk, F. T cells out of control—impaired immune regulation in the inflamed joint. *Nat. Rev. Rheumatol.* **9**, 34–42 (2013).
22. Ohkura, N. *et al.* T cell receptor stimulation-induced epigenetic changes and Foxp3 expression are independent and complementary events required for T_{reg} cell development. *Immunity* **37**, 785–799 (2012).
23. Feuerer, M. *et al.* Genomic definition of multiple *ex vivo* regulatory T cell subphenotypes. *Proc. Natl. Acad. Sci. USA* **107**, 5919–5924 (2010).
24. Zaiss, M.M. *et al.* T_{reg} cells suppress osteoclast formation: a new link between the immune system and bone. *Arthritis Rheum.* **56**, 4104–4112 (2007).
25. Sato, K. *et al.* Th17 functions as an osteoclastogenic helper T cell subset that links T cell activation and bone destruction. *J. Exp. Med.* **203**, 2673–2682 (2006).
26. Ghoreschi, K. *et al.* Generation of pathogenic T_H17 cells in the absence of TGF-β signalling. *Nature* **467**, 967–971 (2010).
27. Lee, Y. *et al.* Induction and molecular signature of pathogenic T_H17 cells. *Nat. Immunol.* **13**, 991–999 (2012).
28. Wu, C. *et al.* Induction of pathogenic T_H17 cells by inducible salt-sensing kinase SGK1. *Nature* **496**, 513–517 (2013).
29. Kleinewietfeld, M. *et al.* Sodium chloride drives autoimmune disease by the induction of pathogenic T_H17 cells. *Nature* **496**, 518–522 (2013).
30. Malhotra, N. *et al.* A network of high-mobility group box transcription factors programs innate interleukin-17 production. *Immunity* **38**, 681–693 (2013).
31. Ramezani-Rad, P. *et al.* SOX4 enables oncogenic survival signals in acute lymphoblastic leukemia. *Blood* **121**, 148–155 (2013).
32. Jordan, M.S. *et al.* Thymic selection of CD4$^+$CD25$^+$ regulatory T cells induced by an agonist self-peptide. *Nat. Immunol.* **2**, 301–306 (2001).
33. Sakaguchi, S., Powrie, F. & Ransohoff, R.M. Re-establishing immunological self-tolerance in autoimmune disease. *Nat. Med.* **18**, 54–58 (2012).
34. Yang, X.P. *et al.* Opposing regulation of the locus encoding IL-17 through direct, reciprocal actions of STAT3 and STAT5. *Nat. Immunol.* **12**, 247–254 (2011).
35. Tang, Q. *et al.* Central role of defective interleukin-2 production in the triggering of islet autoimmune destruction. *Immunity* **28**, 687–697 (2008).
36. Samson, M. *et al.* Inhibition of IL-6 function corrects Th17/T_{reg} imbalance in rheumatoid arthritis patients. *Arthritis Rheum.* **64**, 2499–2503 (2012).
37. Nadkarni, S., Mauri, C. & Ehrenstein, M.R. Anti–TNF-α therapy induces a distinct regulatory T cell population in patients with rheumatoid arthritis via TGF-β. *J. Exp. Med.* **204**, 33–39 (2007).
38. Nie, H. *et al.* Phosphorylation of FOXP3 controls regulatory T cell function and is inhibited by TNF-α in rheumatoid arthritis. *Nat. Med.* **19**, 322–328 (2013).
39. Viatte, S. *et al.* Genetics and epigenetics of rheumatoid arthritis. *Nat. Rev. Rheumatol.* **9**, 141–153 (2013).

ONLINE METHODS

Mice. Mice were kept under specific pathogen–free conditions, and all animal experiments were performed with the approval of the Institutional Review Board at the University of Tokyo. B6.SJL (CD45.1$^+$) and IL-17–GFP knock-in mice were obtained from the Jackson Laboratory and BIOCYTOGEN, respectively. *Foxp3*^{hCD2} knock-in mice[11], Foxp3-GFP-Cre mice[7], ROSA26-loxP-Stop-loxP-YFP reporter mice[19], *Il17a*$^{-/-}$ mice[40] mice and *Tnfsf11*$^{flox/flox}$ mice[41] were described previously. 8- to 12-week-old sex-matched mice were used for experiments unless otherwise mentioned.

Analysis of T cells in the synovium of subjects with RA or osteoarthritis. Human synovial tissue specimens were obtained from subjects undergoing joint replacement surgery or synovectomy at the Tokyo University Hospital. All the subjects with RA fulfilled the 2010 American College of Rheumatology–European League Against Rheumatism criteria for the classification of RA and provided written informed consent. This study was approved by the Institutional Review Board at The University of Tokyo. The tissue was digested with type II collagenase (1 mg ml^{-1}; Worthington) for 2 h at 37 °C. After being filtered, cells were stimulated with phorbol myristate acetate and ionomycin for 5 h. After fixation, cells were examined for the expression of Foxp3, IL-17, CD3 and CD4. Synovitis activity was evaluated macroscopically by the redness and proliferative status of the synovium membrane.

Induction of CIA. We performed CIA in 8- to 12-week-old male C57BL/6J and DBA/1J mice. Mice were immunized with an emulsion consisting of 50 µl of chicken type II collagen (Sigma-Aldrich; 4 mg ml^{-1}) and 50 µl of adjuvant given intradermally into the base of the tail at two sites. For the DBA/1 mice, we added heat-killed *Mycobacterium tuberculosis* H37Ra (Difco Laboratories; 5.0 mg ml^{-1}) in incomplete Freund's adjuvant (Difco Laboratories). For B6 mice, we added H37Ra (3.3 mg ml^{-1}) in complete Freund's adjuvant (CFA) (Difco Laboratories). Three weeks after the primary immunization, mice were challenged with the same collagen and CFA emulsion as the primary immunization. We judged the development of arthritis in the joint using the following criteria: 0, no joint swelling; 1, swelling of one finger joint; 2, mild swelling of the wrist or ankle; or 3, severe swelling of the wrist or ankle. The scores for all fingers of forepaws and hindpaws, wrists and ankles were totaled for each mouse (with a maximum possible score of 12 for each mouse).

T cell isolation and sorting. Single-cell suspensions were obtained from peripheral LNs and the spleen. Splenic erythrocytes were eliminated with red blood cell lysis buffer (Sigma-Aldrich). To purify the peripheral CD4$^+$ T cell subpopulation obtained from *Foxp3*^{hCD2} mice, the pooled spleen and LN cells were subjected to a depletion of any adherent cells by panning with goat anti-mouse IgG Fc (Cappel, 55472, 1:200) and stained with phycoerythrin (PE)-conjugated mouse anti-human CD2 (RPA-2,10, eBiosicence, 1:100). Cells were then incubated with anti-PE microbeads (Milteny Biotech) and separated on LS columns (Milteny Biotech). The hCD2$^+$ or hCD2$^-$ cells were further stained with anti-CD4 and other monoclonal antibodies and subjected to FACS sorting using FACSAriaIII (BD Biosciences). The purity of the sorted cells was >99.9%. The sorted cells were subsequently subjected to cell culture or adoptive transfer experiments. Adoptive transfer was achieved by a tail vein injection of 5×10^5 cells into the collagen-immunized mice 1 d before secondary immunization. For CFSE labeling, cells were stained with 5 µM CFSE (Dojindo) diluted in 0.1% BSA at 37 °C for 10 min.

T cell differentiation *in vitro*. T cells were cultured in Iscove's modified Dulbecco's medium (Sigma-Aldrich) supplemented with 2 mM L-glutamine, 10% FBS, 50 µM 2-ME, 100 U ml^{-1} penicillin and 100 µg ml^{-1} streptomycin. The following reagents were used at the concentrations indicated: 5 µg ml^{-1} anti–IFN-γ (XMG1.2, BD Biosciences), 5 µg ml^{-1} anti–IL-4 (11B11, BD Biosciences), 10 µg ml^{-1} anti–IL-6 (MP5-20F3, eBioscience), 10 µg ml^{-1} anti–TNF-α (1F3F3D4, eBioscience), 10 µg ml^{-1} anti–IL-1β (B122, eBioscience), 10 ng ml^{-1} recombinant mouse IL-1β (rmIL-1β) (R&D Systems), 10 ng ml^{-1} rmIL-2 (R&D Systems), 100 ng ml^{-1} rmIL-6 (PeproTech), 10 ng ml^{-1} rmIL-12 (PeproTech), 10 ng ml^{-1} recombinant human transforming growth factor-β1 (rhTGF-β1) (R&D Systems) and 50 ng ml^{-1} IL-23 (R&D Systems). For T cell stimulation, the sorted T cells were stimulated beads coated with monoclonal antibodies to CD3 and CD28 (Dynal; 25 µl per 1×10^6 cells) for 3 d. For T_H1 cell polarization, naive CD44^{lo}CD62L^{hi}Foxp3^{hCD2-}CD4$^+$ T cells were stimulated in the presence of rmIL-12 and anti–IL-4. For T_H17 cell polarization, naive CD4$^+$ T cells were stimulated in the presence of rmIL-1β, rmIL-6, rmIL-23, rhTGF-β, anti–IFN-γ and anti–IL-4. Naive CD4$^+$ T cells stimulated in the presence of anti–IFN-γand anti–IL-4 were used as T_H0 cells. Foxp3^{hCD2+}CD4$^+$ T cells stimulated in the presence of IL-2 were used as Foxp3$^+$ T cells. For the coculture with synovial fibroblasts, synovial cells (1×10^4 cells per well) were cultured for 1 d before coculture using 96-well flat-bottom plates. The sorted T cells (1×10^5 cells per well) and beads coated with monoclonal antibodies to CD3 and CD28 were added to the culture of synovial fibroblasts. For transwell assays, synovial fibroblasts (6×10^4 cells per lower well) and T cells (1.5×10^5 cells per upper well) were cocultured using 0.4-µm-pore 24-well transwell plates (Coster) in the presence of beads coated with monoclonal antibodies to CD3 and CD28.

Type II collagen–specific response. Titers of collagen-specific antibodies in the serum were measured by ELISA using the SBA Clonotyping System (SouthernBiotech). For the T cell proliferative response, CD25^{hi}Foxp3$^+$CD4$^+$ and CD25^{lo}Foxp3$^+$CD4$^+$ T cell populations were sorted from dLNs and spleens of collagen-immunized mice 10 d after immunization. Purified cells were labeled with CFSE and cultured (1×10^5 per well) in the presence of denatured type II collagen (100 µg ml^{-1}), IL-2 (10 ng ml^{-1}) and Thy1.2-depleted, mitomycin C (Sigma-Aldrich)-treated splenocytes (4×10^5 per well) using 96-well U-bottom plates for 3 d.

Preparation of arthritic synovial fibroblasts. Synovial tissues from the ankles of mice with CIA were minced and digested by type II collagenase (1 mg ml^{-1}; Worthington) in DMEM (Sigma-Aldrich) for 2 h and then cultured in DMEM containing 20% FBS. To prepare *Tnfsf11*$^{Δ/Δ}$ arthritic synovial fibroblasts, *Tnfsf11*$^{Δ/Δ}$ mice were administered 2 mg of antibody to type II collagen (Chondrex) intravenously on day 0 and 50 µg of lipopolysaccharide intraperitoneally on day 3. Cultured fibroblasts during the fourth to seventh passages were used for the experiments. Thy1$^+$CD11b$^-$ synovial fibroblasts and Thy1$^-$CD11b$^+$ synovial macrophages were sorted by FACSAriaIII.

Flow cytometry. Antibodies conjugated with biotin, FITC, Alexa Fluor 488, PE, PerCP-Cy5.5, allophycocyanin (APC), Alexa Fluor 647, eFluor 450 or V500 were used at a 1:100 dilution unless otherwise mentioned. The following monoclonal antibodies were purchased from eBioscience: anti-human CD2 (RPA-2,10), CD3 (OKT3), CD4 (OKT4), FOXP3 (236A/E7), IL-17A (eBio64DEC17), anti-mouse CD3ε (145-2C11), CD4 (RM4-5), CD11b (also called ITGAM) (M1/70), CD25 (PC61), CD39 (24DMS1), CD44 (IM7), CD45.1 (also called PTPRC) (A20), CD45.2 (104), CD62L (also called SELL) (MEL-14), CD90.2 (also called THY1) (53-2.1), CD103 (2E7), OX40 (also called CD134) (OX-86), GITR (also called CD357) (DTA-1, 1:1600), T cell receptor-β (TCR-β) (H57-597), CCR6 (140706), RANKL (IK22/5), KLRG1 (2F1), FR4 (eBio12A5, 1:400), Foxp3 (FJK-16s), CTLA-4 (UC10-4B9), Ki-67 (B56), IFN-γ (XMG1.2), IL-4 (11B11) and IL-17A (eBio17B7). Anti-Helios (22F6) was purchased from BioLegend. Goat anti-mouse/rat Nrp1(FAB566N, 1:40) was purchased from R&D Systems. For intracellular Foxp3 staining, the Foxp3 Staining Buffer Set (eBioscience) was used. For intracellular cytokine staining, cells were stimulated with 50 ng ml^{-1} phorbol myristate acetate (Sigma-Aldrich), 500 ng ml^{-1} ionomycin (Sigma-Aldrich) and GolgiPlug (BD Biosciences) for 5 h. After washing, cells were stained for surface antigens, fixed with 4% paraformaldehyde (Nacalai Tesque) for 10 min at room temperature, permeabilized and stained with monoclonal antibodies to cytokine diluted in Perm/Wash Buffer (BD Biosciences). For the measurement of cytokine concentration in the culture supernatants, BD Cytometric Bead Array was performed. Flow cytometric analysis was performed by FACSCanto II with Diva software (BD Biosciences).

CpG methylation analysis by bisulfite sequencing. After sodium bisulfite treatment (MethylEasy Xceed, Human Genetic Signatures) of genomic DNA, modified DNA was amplified by PCR and subcloned into pUC118 Hinc 2/ BAP (Takara). PCR primers for the *Foxp3* intron 1, *Ctla4* exon 2 and *Il2ra* intron 1a regions were described previously[22].

***In vitro* assay of osteoclast differentiation.** Primary bone marrow cells were suspended in culture medium (α-MEM containing 10% FBS) supplemented with 10 ng ml^{-1} macrophage colony-stimulating factor (M-CSF) (R&D Systems) for 2 d to obtain BMMs. For a coculture of BMMs and T cells, BMMs (5×10^4 cells per well) were cultured with sorted T cells (1×10^5 cells per well) in the presence of 10 ng ml^{-1} M-CSF and beads coated with monoclonal antibodies to CD3 and CD28 for 7 d using a 96-well flat-bottom plate, and TRAP$^+$ MNCs (more than three nuclei) were counted. For a coculture of BMMs, synovial fibroblasts and T cells, BMMs (5×10^4 per well) and sorted T cells (1×10^5 or 5×10^4 cells per well) were cocultured with synovial fibroblasts (1×10^3 per well), which were isolated and cultured 1 d before coculture. Coculture was performed in the presence of beads coated with monoclonal antibodies to CD3 and CD28. After 5 d, TRAP$^+$ MNCs were counted.

Analysis of bone phenotype. The histomorphometric analysis has been described previously[41]. The articular cartilage dysfunction score was calculated by the ratio of the toluidine blue–negative area to the total articular cartilage area. For the microcomputed tomography analysis, calcaneus in the ankle joints of arthritic mice 5 weeks after secondary immunization was subjected to three-dimensional microcomputed tomography. Computed tomography scanning was performed using a ScanXmate-A100S Scanner (Comscantechno). Three-dimensional microstructural image data were reconstructed, and structural indices were calculated using TRI/3D-BON software (RATOC).

GeneChip analysis. The GeneChip analysis was performed as described previously[42]. IL-17^{GFP+}Foxp3^{hCD2-} cells differentiated from Foxp3^{hCD2+}CD4$^+$ cells under T_H17-polarizing conditions for 4 d were sorted and used as exFoxp3 T_H17 cells. IL-17^{GFP+}Foxp3^{hCD2-} cells differentiated from naive CD4$^+$ cells under T_H17-polarizing conditions were used as T_H17 cells. IL-17^{GFP-}Foxp3^{hCD2+} cells after the culture of Foxp3^{hCD2+}CD4$^+$ cells in the presence of IL-2 were used as T_{reg} cells. T_H0 cells were also used for this analysis. $8–10 \times 10^5$ cells of each T cell subset after culture were subsequently subjected to RNA extraction. The total RNAs extracted from these cells were used for cDNA synthesis by reverse transcription, followed by synthesis of biotinylated cRNA through *in vitro* transcription. After cRNA fragmentation, hybridization with the Mouse Genome 430 2.0 Array (Affymetrix) was performed as described previously[42]. The main part of the data set was deposited and can be obtained from the Genome Network Platform (http://genomenetwork.nig.ac.jp/). We performed microarray analysis using three sets of T cell samples that were independently prepared from 16–18 IL-17^{GFP} *Foxp3*^{hCD2} mice (51 mice in total). The microarray data have been deposited in the Gene Expression Omnibus database with accession code GSE48428.

Statistical analyses. Statistical analyses were performed using one-way analysis of variance with Newman-Keuls multiple comparison test and unpaired two-tailed Student's *t* test (*$P < 0.05$, **$P < 0.01$, ***$P < 0.005$; NS, not significant; ND, not detected in all figures). All data are expressed as the mean ± s.e.m. The results are representative examples of more than three independent experiments. We estimated the sample size considering the variation and mean of the samples. We tried to reach the conclusion using as small a size of samples as possible. We usually excluded samples if we observed any abnormality in terms of size, weight or apparent disease symptoms in mice before performing experiments. However, we did not exclude animals here, as we did not observe any abnormalities in the present study. Neither randomization nor blinding was done in this study. Statistical tests are justified as appropriate for every figure, and the data meet the assumptions of the tests.

40. Nakae, S. *et al.* Antigen-specific T cell sensitization is impaired in IL-17–deficient mice, causing suppression of allergic cellular and humoral responses. *Immunity* **17**, 375–387 (2002).
41. Nakashima, T. *et al.* Evidence for osteocyte regulation of bone homeostasis through RANKL expression. *Nat. Med.* **17**, 1231–1234 (2011).
42. Takayanagi, H. *et al.* Induction and activation of the transcription factor NFATc1 (NFAT2) integrate RANKL signaling in terminal differentiation of osteoclasts. *Dev. Cell* **3**, 889–901 (2002).

doi:10.1038/nm.3432